Structural and dynamical consequences of density variation in vitreous silica

2003 J. Phys.: Condens. Matter 15 S995

(http://iopscience.iop.org/0953-8984/15/11/322)

INSTITUTE OF PHYSICS PUBLISHING JOURNAL OF PHYSICS: CONDENSED MATTER

J. Phys.: Condens. Matter **15** (2003) S995–S1005 PII: S0953-8984(03)58216-9

Structural and dynamical consequences of density variation in vitreous silica

O Pilla[1,3], L Angelani[2], A Fontana[1], J R Gonçalves[1,4] and G Ruocco[2]

[1] INFM and Dipartimento di Fisica, Università di Trento, 38050 Povo, Trento, Italy
[2] INFM and Dipartimento di Fisica, Università di Roma La Sapienza, 00185 Roma, Italy

E-mail: pilla@science.unitn.it

Received 24 October 2002
Published 10 March 2003
Online at stacks.iop.org/JPhysCM/15/S995

Abstract

We present structural and dynamical results of molecular dynamics simulation of vitreous silica undergoing a hydrostatic compression and decompression cycle at room temperature. Structural results as a function of density compare fairly well with experiments as well as with the longitudinal and transverse sound velocity pressure dependence. A shift of the boson peak (BP) toward higher energies and its simultaneous weakening is observed as in experiments. A detailed study of the dispersion of the glass vibration is presented at several densities and for the densified state. Evidence of phonon-like character with two distinct pseudo-periods is shown for longitudinal and transverse dynamics. The relationship between the BP vibrations and the correlation length scale indicated by the first sharp diffraction peak is discussed.

1. Introduction

The characterization of vibrations in disordered systems is a very intriguing task [1]. In disordered systems in fact, the usual crystal-like phonon theory is in principle no longer valid. This implies that the existence of a dispersion relationship between the vibrational energy E and its wavevector Q cannot be postulated *a priori* and that Q is no longer a good quantum number.

One can, also in disordered solids, consider two limiting cases where the characterization of the vibrations is unquestionable. The first is that of very long-wavelength (small-Q) vibrations, which are rather insensitive to the microscopic disorder, their wavelength being much longer than its characteristic length scale. These vibrations behave like plane waves and can safely be considered as phonon-like. The second case is that of very short wavelength,

[3] Author to whom any correspondence should be addressed.
[4] Permanent address: Departamento de Física, Universidade Federal do Ceará, CP 6030, Campus do Pici, 60455-760 Fortaleza, Ceará, Brazil.

0953-8984/03/110995+11$30.00

i.e. very high wavevector $\boldsymbol{Q}$, which are greatly affected by the local disorder and lose any phonon-like character, becoming localized and non-propagating waves.

Except for these particular cases, the general discussion on the character of the vibrations in the mesoscopic range in amorphous materials is still open, and several, sometimes contrasting, hypotheses have been made on their nature. In particular, up to now, the question of whether vibrations in the mesoscopic energy range could be correctly considered as phonon-like or rather treated as non-propagating or localized waves [2–5] has not yet received a convincing answer.

In a wide series of glasses the phonon-like behaviour of these vibrations has been experimentally demonstrated by means of x-ray Brillouin measurements and verified with computer simulation [6–9], which supports the phonon-like picture. In the case of vitreous (v-SiO_2), this question remains open and two different interpretations are proposed. Recently experimental x-ray Brillouin results on v-SiO_2 [10, 11] have directly shown the existence of a well defined dispersion relation for vibrations whose energies are of the order of several millielectronvolts [10, 12]. These energies are much higher than the maximum energy of the boson peak (BP), i.e. the excess, in the Debye sense, of vibrational states, which is characteristic of amorphous materials. On the other hand, x-ray Brillouin [13] and enhanced Raman spectra [14] of densified v-SiO_2($\rho = 2.67$ g cm^{-3}) have been interpreted considering the BP energy as the limit between propagating and non-propagating vibrations.

In this paper we present computer simulation studies of v-SiO_2 at different densities, reproducing a typical room temperature hydrostatic pressure experiment. The density is stepwise raised from the nominal value of 2.2 g cm^{-3}, typical of normal v-SiO_2, to 4.2 g cm^{-3}, and subsequently decreased. By monitoring the pressure of simulations we obtain a densified v-SiO_2 sample with $\rho = 2.8$ g cm^{-3} at the end of the cycle. Structural and dynamical variations with density have been monitored and are presented. Phonon-like dispersion relations have been found to dominate the dynamical structure factor, $S(Q, E)$. The possible relationship between BP and the first sharp diffraction peak (FDSP) length scale is also discussed.

2. Simulation details

The effects of density variation on v-SiO_2 have been the object of several experimental studies as well as computer simulation investigations. Computer simulations using the three-body van Beest [15] potential have been presented by Jin *et al* [16], who studied the compression of SiO_2 up to 4.28 g cm^{-3}. Other authors also studied the dynamics of vitreous silica at different densities with the use of several *ab initio* potentials [17–20]. Here we propose a protocol which is appropriate to compare directly to hydrostatic pressure experiments using the two-body van Beest potential [15]. The long-range interactions were treated by the Ewald-sum technique.

The system, made up of 680 SiO_2 molecules ($N = 2040$ ions) at 5000 K, $\rho = 2.2$ g cm^{-3}, in the liquid state, was equilibrated for a long time, and then slowly cooled down to 300 K with the use of molecular dynamics. The further computational steps were as follows:

(i) conjugate gradient search for minimum configuration corresponding to that density;
(ii) diagonalization of the dynamical matrix to obtain the eigenfrequencies and eigenvectors (assuming the harmonic approximation);
(iii) varying the density by about 1.5% and going to step (i).

Steps (i)–(iii) were repeated up to a density of 4.2 g cm^{-3}, and then the density was lowered in the same way. The density variation was obtained by scaling the simulation box length. For each minimum configuration we computed the relative pressure using the virial theorem.

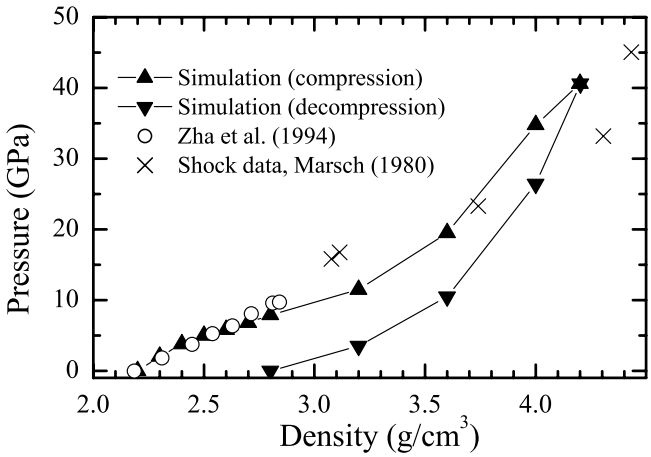

Figure 1. Pressure–volume relation for v-SiO_2: full triangles, present study compared with the experiments; open circles, diamond anvil cell data by Zha *et al* [25]; crosses, shock data by Marsch [26]. Up and down triangles refer to compression and decompression cycles respectively.

The descent in the density was stopped when a box length corresponding to zero pressure was reached.

From the equilibrium configurations at various densities we computed the calculation of the static structure factor, the pair correlation function and the interatomic distances as well as the bond angles. From the eigenvectors and their eigenvalues, we calculated the dynamical structure factor, $S(Q, E)$, for longitudinal and transverse vibrations [11, 21, 22], to compare with experiments and the corresponding currents $C_i(Q, E) = S_i(Q, E)Q^2/E^2$, where i stands for L (longitudinal) and T (transverse) respectively, which contain the relevant dynamical information. The sound velocities, both longitudinal and transverse, were estimated from the lowest energy eigenvalues and eigenvectors.

3. Test of the model

The quality of the van Beest potential in describing both the structural and dynamical properties of v-SiO_2 at $\rho = 2.2$ g cm^{-3} has been demonstrated by several authors [21–23], but up to now, density studies were carried out using three-body [16] or *ab initio* potentials [17, 19, 20, 24]. The density–pressure diagram deduced by the present simulation is shown in figure 1 and compared with available experimental data. The agreement is rather good, especially in the low-density region where anvil cell measurements are available [25]. In the high-density region the comparison is possible only with the less accurate shock wave data [26]. In figure 2 we report the longitudinal and transverse sound velocity dependence on pressure as obtained in the present simulation, full symbols, and those measured by Zha and co-workers [25], open symbols. The agreement is quasi-quantitative, except for a few pressures in the descending cycle. The hysteretic behaviour, the onset of densification at $P > 12$ GPa and the initial decrease of the velocities with increasing pressure are well accounted for by the model as well as the density of the sample obtained after the compression–decompression run. The dispersion curves from which the sound velocities have been derived show a linear character up to several tenths of a millielectronvolt except for the lowest-density samples where an anomalous dispersion is observed [11]. In these cases we considered the velocity of sound relative to the low Q–E range. The static structure factor is shown in figure 3. Here also the

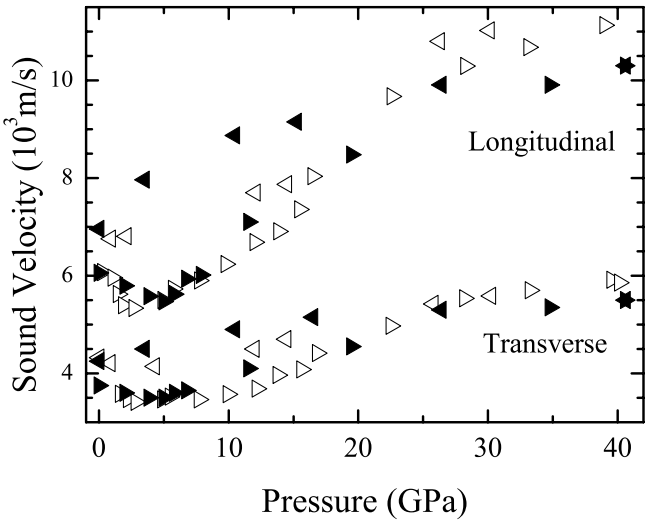

Figure 2. Sound velocities of v-SiO_2 as a function of pressure. Solid triangles, present simulations; open triangles, experimental data taken from Zha *et al* [25]. Right and left triangles refer to compression and decompression cycles respectively.

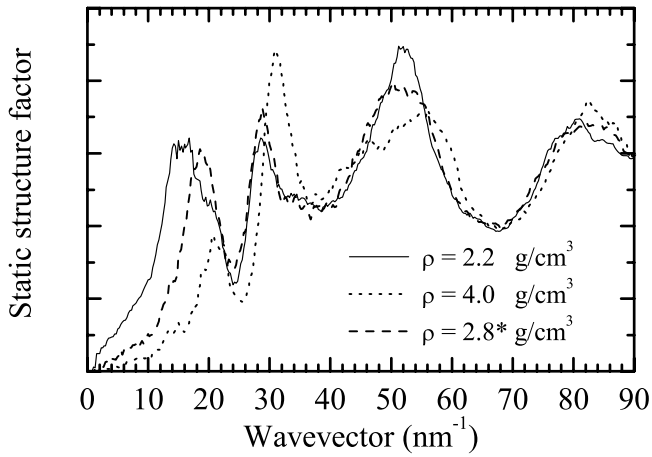

Figure 3. Neutron static structure factor computed for vitreous silica at three different densities. The asterisk refers to the decompression cycle.

model reproduces satisfactorily both the intensities and the shifts of the first two peaks with density [27, 28].

All these observations make us confident in the quality of the used potential in describing both structural and dynamical properties of v-SiO_2 as a function of the density.

4. Results

4.1. Structural results

In table 1 we report the mean nearest-neighbour interatomic distances d_{Si-O}, d_{Si-Si} and d_{O-O}, obtained from simulation at various densities. The asterisks refer to the densities in the descending run (on decompression). At densities higher than 2.8 g cm^{-3}, both d_{Si-O} and

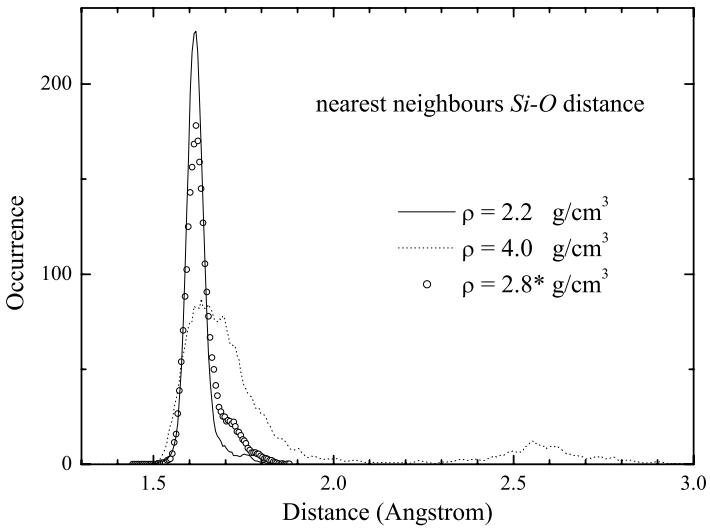

Figure 4. Si–O nearest-neighbour interatomic distance distribution for $\rho = 2.2$ g cm^{-3} (full curve), $\rho = 4.0$ g cm^{-3} (dotted curve) and $\rho = 2.8^*$ g cm^{-3} (open circles).

Table 1. Nearest-neighbour silicon–oxygen, oxygen–oxygen and silicon–silicon computed mean distances (Å), at various densities (g cm^{-3}). The densities corresponding to the decompression cycle are marked by asterisks. Figures in parentheses give the relative intensity of the two peaks observed in the pair correlation.

ρ	d_{Si-O}		d_{O-O}		d_{Si-Si}
2.2	1.620		2.615		3.113
2.3	1.615		2.609		3.088
2.4	1.611		2.603		3.064
2.5	1.609		2.599		3.044
2.6	1.608		2.595		3.042
2.7	1.607		2.593		3.030
2.8	1.606		2.589		3.022
3.2	1.606 (58%)	1.685 (42%)	2.572	2.669 (16%)	3.046 (84%)
3.6	1.605 (30%)	1.683 (70%)	2.537	2.636 (21%)	3.059 (79%)
4.0	1.615 (27%)	1.692 (73%)	2.487	2.619 (26%)	3.064 (74%)
4.2	1.676		2.465	2.638 (29%)	3.078 (71%)
4.0*	1.682		2.500	2.654 (27%)	3.105 (73%)
3.6*	1.666		2.553	2.673 (21%)	3.120 (79%)
3.2*	1.629		2.595	2.721 (17%)	3.126 (83%)
2.8*	1.623		2.614		3.118

d_{Si-Si} are two valued, indicating the coexistence of tetrahedrally and octahedrally coordinated Si atoms. This, as already observed by Jin *et al* [16], indicates that increasing density in v-SiO_2 results in a progressive transition from a cristobalite-like local structure, which is tetrahedrally coordinated, to an octahedral stishovite-like one [29]. In figure 4 the mean nearest-neighbour interatomic distances, d_{Si-O}, are shown for three selected densities. The broad feature located at about 2.6 Å in the $\rho = 4.0$ g cm^{-3} sample indicates that the transition to octahedral sixfold coordination is not completed at this density.

The Si–Ô–Si mean bond angle shows in the same density range a double-peak structure with maxima at around 130° and 100°, instead of the $\rho = 2.2$ g cm^{-3} value of 144°. On

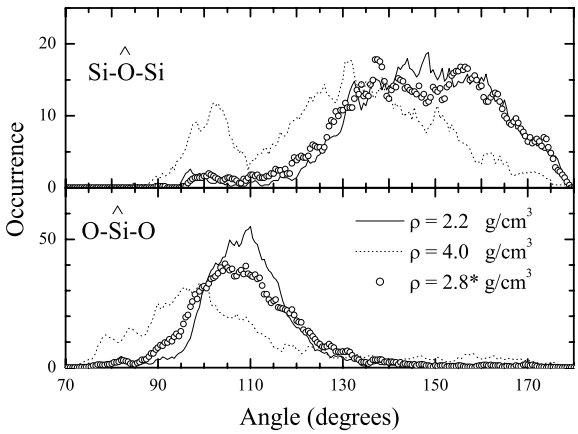

Figure 5. Si–Ô–Si (upper) and O–Ŝi–O (lower) bond angle distribution for $\rho = 2.2$ g cm^{-3} (full curve), $\rho = 4.0$ g cm^{-3} (dotted curve) and $\rho = 2.8^*$ g cm^{-3} (open circles).

the other hand, the O–Ŝi–O angle shifts in the same density range from 110° to 95°. The distribution of Si–Ô–Si and O–Ŝi–O angles is reported in figure 5 for the same densities as shown in figure 4. In the expansion run, corresponding to the densities marked by asterisks in table 1, the octahedral symmetry progressively disappears and is completely absent in the densified sample, $\rho = 2.8$ g cm^{-3}, where both distances and mean bond angles are compatible with a tetrahedral environment of the Si atoms.

This observation has two consequences:

(i) the pressure-induced tetrahedral to octahedral phase transition is reversible up to $\rho = 4.2$ g cm^{-3};
(ii) the densified sample with $\rho = 2.8$ g cm^{-3} has tetrahedral symmetry as the starting one.

Thus the densification involves the medium-range ordering of tetrahedra rather than the short-range environment of Si ions [11]. This latter conclusion is also in agreement with the position of the FSDP, which greatly shifts toward higher wavevectors with compression, figure 3, and at the same time decreases in intensity. Since the presence of the FDSP has been ascribed to the medium-range ordering [30], its shift (from 16 to 21 nm^{-1}) indicates the variation of the corresponding structural period toward smaller distances during compression, while its weakening can be ascribed to a progressive disappearance of the correlation length. These effects on the FDSP are partly reversible as are those observed on bond lengths and bond angles, being only slightly shifted and weaker in the $\rho = 2.8^*$ g cm^{-3} realization than in the starting one ($\rho = 2.2$ g cm^{-3}).

4.2. Dynamical results

The dynamical effects of compression and subsequent decompression are not limited to the cited sound velocity variation. In figure 6, the densities of states, $g(E)$, relative to the realizations at $\rho = 2.2$, 4.0 and 2.8* g cm^{-3} are shown. Compression results in an overall shift of vibrational modes toward higher energies, which is almost completely recovered after decompression. Moreover, the gap between the highest-frequency optical branches, located at $E > 120$ meV, has almost disappeared at the highest density. The BP as a function of density is reported in the inset of figure 6, where the quantity $g(E)/E^2$ is plotted versus energy. As it can be seen from the figure, the compressed sample shows a very small excess of states, which is

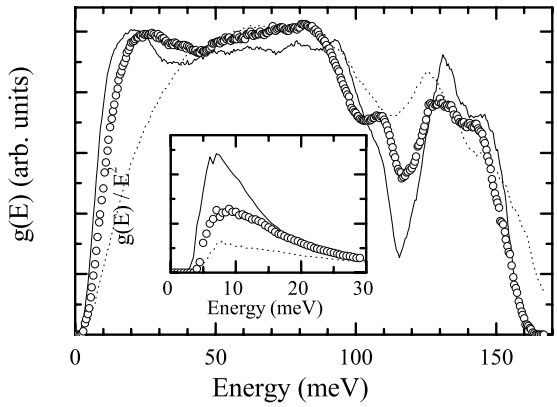

Figure 6. Vibrational density of states of v-SiO_2 at $\rho = 2.2$ g cm^{-3} (full curve), $\rho = 4.0$ g cm^{-3} (dotted curve) and $\rho = 2.8^*$ g cm^{-3} (open circles). In the inset is reported the low-energy part of $g(\omega)/\omega^2$ showing the the BP density dependence.

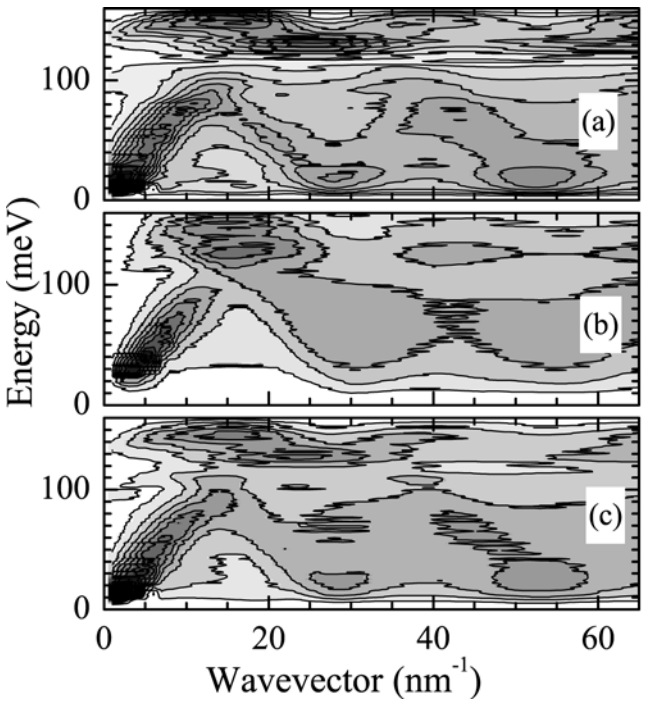

Figure 7. Computed longitudinal current grey scale maps for v-SiO_2 at three different densities relative to neutron scattering: (a) $\rho = 2.2$ g cm^{-3}; (b) $\rho = 4.0$ g cm^{-3} (compression); (c) $\rho = 2.8^*$ g cm^{-3} (decompression). The currents have been divided by Q^2 in order to better visualize the details.

only partly recovered in the densified realization, after decompression. It is worth noting that experimentally the BP intensity has been found to lower both in *in situ* measurements [27], and in the permanently densified v-SiO_2 samples [31–33].

The dispersion relations relative to the longitudinal and transverse vibrational dynamics for $\rho = 2.2$, 4.0 and 2.8^* g cm^{-3} realizations are reported in figures 7 and 8, respectively.

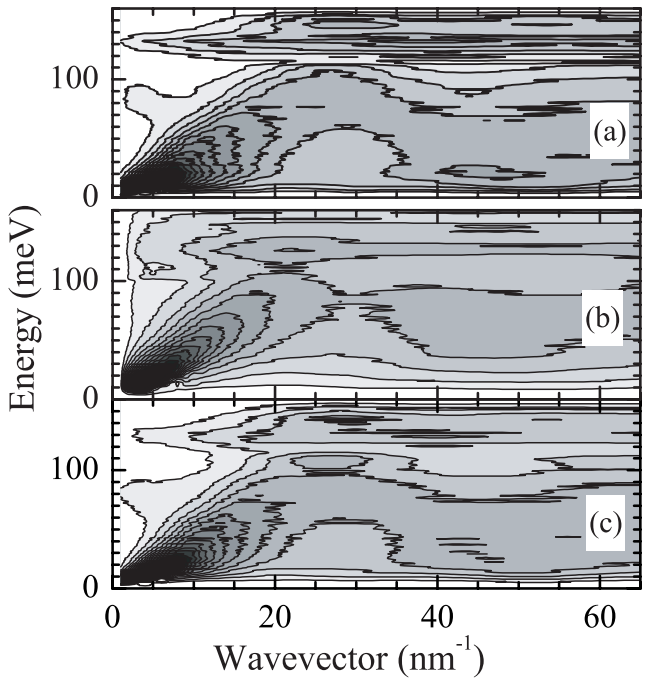

Figure 8. The same as figure 7 but for the transverse currents.

Actually, in both figures the quantities plotted in a grey-scale map are $C_L(Q, E)/Q^2$ and $C_T(Q, E)/Q^2$, respectively. The division by the Q^2 factor has been done in order to extract the trivial Q^2-dependence and better visualize the structures in the current maps, and it does not modify their energy dependence. Figures 7(a) and 8(a) cover a more extended Q-region than those reported by Taraskin and Elliott [22], who draw a dispersion relation for longitudinal and transverse vibrations reporting the position of the maxima in the currents up to 38 nm^{-1}. In a perfect crystal these maps should contain the periodic phonon dispersion relations for vibrations propagating in the various crystallographic directions. It is worth noting that even in a glassy material like v-SiO_2 at normal density, a trace of periodicity is also present in the highest optical modes ($E > 120$ meV). In particular, in the acoustic energy region a marked wavy trace is clearly observable with a quasi-period of about 28 nm^{-1} for longitudinal vibrations and about 50 nm^{-1} for the transverse ones. In the compressed sample with $\rho = 4.0$ g cm^{-3} (figures 7(b) and 8(b)) this trace is still observable, even if rather weaker. The quasi-periods are at this density of $\sim$31 and $\sim$50 nm^{-1} for C_L and C_T, respectively. Finally, the permanently densified sample shows (figures 7(c) and 8(c)) an intermediate behaviour, both concerning the evidence of the periodic structure and the quasi-periods, which are however very close to those of the starting realization.

In all the studied densities the current maps show a rather defined periodicity, implying an underlying and significant phonon-like character of the involved vibrations, especially in the region of the first pseudo-Brillouin zone. In fact, in that range the periodic part is rather well defined and relatively sharp up to energies of the order of tenths of a millielectronvolt. The periodicity is then progressively wiped out by compression and restored by decompression. As far as the pseudo-periodicity is concerned, it is easy, by comparing the current maps of figures 7 and 8 with the statical structure factors for the three densities of figure 3, to observe

that the longitudinal currents show a pseudo-periodicity corresponding to the position of the second peak in $S(Q)$, while the periodicity of the transverse currents is that of the third peak in $S(Q)$. The density dependence of the position of these two structures in $S(Q)$ also fits very well with the density variation of the current pseudo-periodicities.

The relation between the pseudo-period observed in the longitudinal dispersion curve and the second peak of $S(Q)$ was proposed early by Taraskin and Elliott [22], who observed that its position was dependent on the height, d, of the SiO_2 tetrahedra. It is easy to verify that, using the bond distances reported in table 1 and the cited O–$\hat{\text{Si}}$–O bond angles, the variation of d will give a shift of the second peak during compression from 29 nm^{-1} at $\rho = 2.2$ g cm^{-3} to 33 nm^{-1} at $\rho = 4.0$ g cm^{-3}. These values fit the computed ones shown in figure 7 very well.

Transverse currents, on the other hand, show a much less marked, if any, variation of pseudo-periodicity with density, which remains fixed at about 50 nm^{-1}. This is the exact position of the third peak in $S(Q)$ (figure 3), which is also insensitive to density and whose origin, at $\rho = 2.2$ g cm^{-3}, is due to Si–Si, Si–O and O–O correlation lengths [16]. The only one of these distances that does not vary appreciably with pressure is Si–O, so we argue that transverse dynamics mainly depends on the Si–O interatomic distance rather than on second-nearest-neighbour geometry. In fact, as can be argued by comparing figures 4 and 5, Si atoms at high density retain to a certain extent a tetrahedral environment where the four oxygen atoms which are closest to Si atoms have a rather regular position. The remaining two oxygen neighbours are located at greater distances and the dispersion of their distances is wider by a factor of three to six than those of the four closest O atoms.

In addition to the pseudo-periodic behaviour in figure 7(a), an intense plateau is present in the (E, Q) region included in between 10 and 30 meV and 5–20 nm^{-1}. In figure 7(a) it appears like a peninsula which originates from the (quasi-) linear dispersion curve in the low-Q–E region, and stays parallel to the x-axis of the figure up to about 20 nm^{-1}. This structure is even more evident in the transverse dynamics (figure 8(a)). In the highest-density sample this structure is absent and is only partially recovered in the $\rho = 2.8^*$ g cm^{-3} permanently densified one. This branch has been assigned to the flattening of the TA branch near the first van Hove singularity [11, 22, 34], and does not show a marked pseudo-periodic behaviour, except for a weak replica around 35–40 nm^{-1} (figure 8(a)).

The presence of this band in the transverse currents and the corresponding 'spilled' structure in the longitudinal ones has been connected to the observation, in the neutron and x-ray inelastic experiments, of peaks in $S(Q, E)$ in that energy–wavevector range [10, 11]. This interpretation is further supported by the fact that these peaks disappear in the simulated current with increasing density, as observed early for the BP.

Since the FSDP intensity also behaves in a very similar way with density, one could, at first, infer that an inter-relationship exists among

(i) the excess of vibrational states giving rise to the BP in the density of states,
(ii) the presence of the van Hove singularity and the consequent flattening of the lowest TA branch and
(iii) the intermediate-range order which is assumed to be responsible for the presence of the FSDP.

The connection between items (i) and (ii) has already been pointed out [11, 22, 34], and the assignment of the BP vibrations to a flattened transverse branch is generally accepted. Their link with the FSDP is much less evident and deserves further discussion. In fact, assuming that the FSDP indicates a correlation length for the excess vibrations in the BP range, in the current spectra one should observe a pseudo-periodicity of the order of 15–20 nm^{-1}, which is not present in the simulations. A possible explanation for the density variation of the FSDP can

rather be found in the progressive disappearance of 'cavities' linked to the ringlike structures, characteristic of v-SiO_2 [11]. The permanent densification would be, in this case, only the consequence of the shrinking of the empty volumes, which do not appreciably alter the local symmetry, being mostly related to the medium-range microscopic disorder.

5. Conclusion

We have shown that v-SiO_2 shows in its vibrational dynamics a marked phonon-like behaviour at all the studied densities. The trace of a dispersion relation is observed well beyond the low-energy and low-wavevector region, where it was early supposed to hold. Two different length scales have been found to dominate the vibrational dynamics: while the longitudinal vibrations are mostly related to the height of SiO_4 tetrahedra, the transverse ones have a pseudo-Brillouin zone border which is probably connected to the Si–O distance.

In addition, strong effects induced by compression and decompression have been found in the density of states, in the BP intensity and in the overall vibrational dynamics. No direct relationship has been observed between the intermediate-range microscopical order, responsible for the presence of the FSDP in the static structure factor, and the excess of the vibrational states in the BP range.

Acknowledgments

This work was supported by INFM Iniziativa di Calcolo Parallelo, and by Murst Progetto di Ricerca di Interesse Nazionale. The financial support by the Italian Ministero degli Affari Esteri is gratefully acknowledged.

References

[1] Fontana A and Viliani G 2002 *8th Int. Workshop on Disordered Systems (Andalo, 2001) Phil. Mag.* B **82** (special issue)
[2] Benassi P, Krisch M, Masciovecchio C, Mazzacurati V, Monaco G, Ruocco G, Sette F and Verbeni R 1996 *Phys. Rev. Lett.* **77** 3835
[3] Benassi P, Krisch M, Masciovecchio C, Mazzacurati V, Monaco G, Ruocco G, Sette F and Verbeni R 1997 *Phys. Rev. Lett.* **78** 4670
[4] Foret M, Courtens E, Vacher R and Suck J B 1996 *Phys. Rev. Lett.* **77** 3831
[5] Foret M, Courtens E, Vacher R and Suck J B 1997 *Phys. Rev. Lett.* **78** 4669
[6] Masciovecchio C, Ruocco G, Sette F, Krisch M, Verbeni R, Bergmann U and Soltwisch M 1996 *Phys. Rev. Lett.* **76** 3356
[7] Sette F, Krisch M H, Masciovecchio C, Ruocco G and Monaco G 1998 *Science* **280** 1550
[8] Fioretto D, Buchenau U, Comez L, Sokolov A P, Masciovecchio C, Mermet A, Ruocco G, Sette F, Willner L, Frick B, Richter D and Verdini L 1999 *Phys. Rev.* E **59** 4470
[9] Sokolov A P, Buchenau U, Richter D, Masciovecchio C, Sette F, Mermet A, Fioretto D, Ruocco G, Willner L and Frick B 1999 *Phys. Rev.* E **60** R2464
[10] Pilla O, Cunsolo A, Fontana A, Masciovecchio C, Monaco G, Montagna M, Ruocco G, Scopigno T and Sette F 2000 *Phys. Rev. Lett.* **85** 2136
[11] Pilla O, Caponi S, Fontana A, Montagna M, Rossi F, Viliani G, Angelani L, Ruocco G, Monaco G and Sette F 2002 *Preprint* cond-mat 0209519
[12] Pilla O, Angelani L, Ruocco G and Freire P T C 2002 *Phil. Mag.* B **82** 223
[13] Foret M, Vacher R, Courtens E and Monaco G 2002 *Phys. Rev.* B **66** 024204
[14] Hehlen B, Courtens E, Vacher R, Yamanaka A, Kataoka M and Inoue K 2000 *Phys. Rev. Lett.* **84** 5355
[15] van Beest B W H, Kramer G J and van Santen R A 1990 *Phys. Rev. Lett.* **64** 1955
[16] Jin W, Kalia R K and Vashishta P 1994 *Phys. Rev.* B **50** 118
[17] Della Valle G and Venuti E 1996 *Phys. Rev.* B **54** 3809
[18] Lacks D J 1998 *Phys. Rev. Lett.* **80** 5385

[19] Lacks D J 2000 *Phys. Rev. Lett.* **84** 4629
[20] Guillot B and Guissani Y 1997 *Phys. Rev. Lett.* **78** 2401
[21] Dell'Anna R, Ruocco G, Sampoli M and Viliani G 1998 *Phys. Rev. Lett.* **80** 1236
[22] Taraskin S N and Elliot S R 1998 *Phil. Mag.* B **2** 403
[23] Vashishta R K, Kalia R K, Rino J P and Ebbsojö I 1990 *Phys. Rev.* B **41** 12197
[24] Wentzcovitch R M, da Silva C and Chelikowsky J R 1998 *Phys. Rev. Lett.* **80** 2149
[25] Zha C S, Hemley R J, Mao H K, Duffy T S and Meade C 1994 *Phys. Rev.* B **50** 13105
[26] Marsch S P 1980 *LASL Shock Hugoniot Data* (Berkeley, CA: University of California Press)
[27] Meade C, Hemley R J and Mao H K 1992 *Phys. Rev. Lett.* **69** 1387
[28] Tan C Z and Arndt J 1999 *J. Non-Cryst. Solids* **249** 47
[29] Grimsditch M, Bhadra R, Meng Y and Hemley R J 1988 *Phys. Rev.* B **38** 7836
[30] Elliott S R 1991 *Phys. Rev. Lett.* **67** 711
[31] Sugai S and Onera A 1966 *Phys. Rev. Lett.* **20** 4210
[32] Inamura Y, Arai M, Yamamuro O, Inaba A, Kitamura N, Otomo T, Matsuo T, Bennington S M and Hanon A C 1999 *Physica* B **263/264** 299
[33] Inamura Y, Arai M, Otomo T, Kitamura N and Buchenau U 2000 *Physica* B **284–288** 1157
[34] Buchenau U, Prager M, Nücker N, Dianoux A J, Ahmad N and Phillips W A 1986 *Phys. Rev.* B **34** 5665